ELSEVIER

Journal of Power Sources 80 (1999) 164–170

JOURNAL OF POWER SOURCES

The ZEBRA electric vehicle battery: power and energy improvements

Roy C. Galloway *, Steven Haslam

Beta Research & Development, Sinfin, Derby DE24 9GN, UK

Received 11 November 1998; accepted 8 December 1998

Abstract

Vehicle trials with the first sodium/nickel chloride ZEBRA batteries indicated that the pulse power capability of the battery needed to be improved towards the end of the discharge. A research programme led to several design changes to improve the cell which, in combination, have improved the power of the battery to greater than 150 W kg^{-1} at 80% depth of discharge. Bench and vehicle tests have established the stability of the high power battery over several years of cycling. The gravimetric energy density of the first generation of cells was less than 100 Wh kg^{-1}. Optimisation of the design has led to a cell with a specific energy of 120 Wh kg^{-1} or 86 Wh kg^{-1} for a 30 kWh battery. Recently, the cell chemistry has been altered to improve the useful capacity. The cell is assembled in the over-discharged state and during the first charge the following reactions occur: at 1.6 V: $Al + 4NaCl = NaAlCl_4 + 3Na$; at 2.35 V: $Fe + 2NaCl = FeCl_2 + 2Na$; at 2.58 V: $Ni + 2NaCl = NiCl_2 + 2\,Na$. The first reaction serves to prime the negative sodium electrode but occurs at too low a voltage to be of use in providing useful capacity. By minimising the aluminium content more NaCl is released for the main reactions to improve the capacity of the cell. This, and further composition optimisation, have resulted in cells with specific energies in excess of 140 Wh kg^{-1}, which equates to battery energies > 100 Wh kg^{-1}. The present production battery, as installed in a Mercedes Benz A class electric vehicle, gives a driving range of 205 km (128 miles) in city and hill climbing. The cells with improved capacity will extend the practical driving range to beyond 240 km (150 miles).

Keywords: Sodium/metal chloride batteries; Applications/electric vehicles; ZEBRA

1. Introduction

The ZEBRA high-energy battery has been tested in cars, buses and light delivery vehicles for more than ten years. In total, more than 2 million km has been travelled in ZEBRA powered vehicles. It became apparent that for the car application an improvement in power was desirable. A new cell was described recently [1] which raised the pulse power of the battery to more than 150 W kg^{-1} throughout the discharge. Current development work indicates the energy of the cell can also be significantly improved to give a battery with an energy density in excess of 100 Wh kg^{-1}.

This paper describes the cell design changes which have produced these performance improvements.

2. Power improvement

The first generation of batteries was produced using SL/09 cells which had cylindrical beta alumina tubes and nickel chloride positive electrodes. During vehicle trials it emerged that a battery power pulse of 150 W kg^{-1} (140 W per cell) was required by passenger vehicles for traffic compatibility. This requirement was not met by SL/09 cells other than in the early stages of discharge, whereas at 80% depth of discharge (DOD) the power pulse available had diminished to 80 W kg^{-1}.

A research program was begun to improve the power of the ZEBRA cell, and the improvement in pulse power from each successive design is described below. These improvements are illustrated in Fig. 1 which shows peak power (2/3 OCV, 30 s) vs. depth of discharge (Ah).

One reason for the power loss was the thickness of the positive electrode at high depths of discharge. To reduce this, a beta alumina tube of cruciform cross-section was produced (Fig. 2). This had the additional advantage of

* Corresponding author

0378-7753/99/$ - see front matter
PII: S0378-7753(98)00259-6

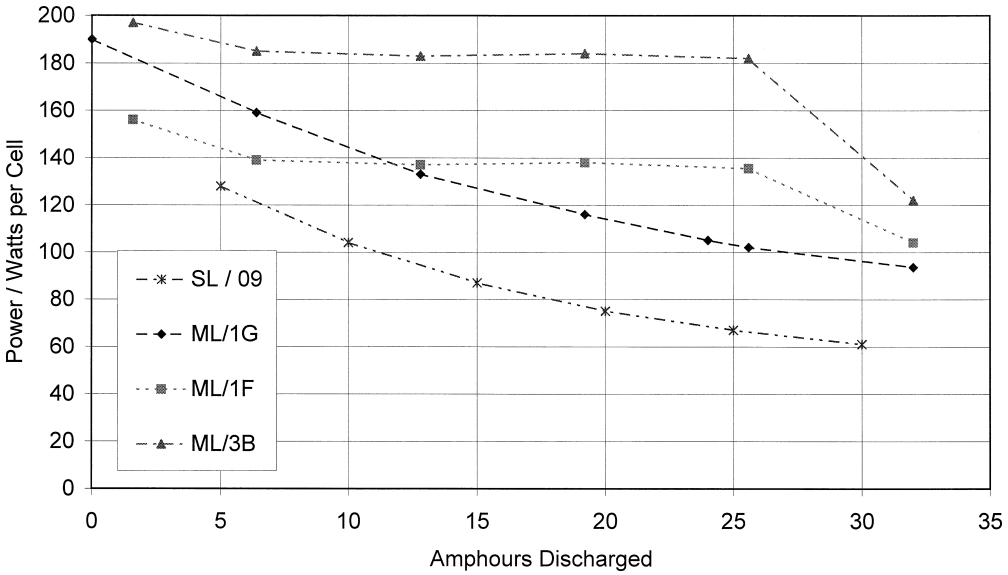

Fig. 1. Plot showing the improvement in peak power performance for ZEBRA cell designs vs. DOD. Pulse power taken at 30 s, 2/3 of OCV. Temperature: 295 to 350°C.

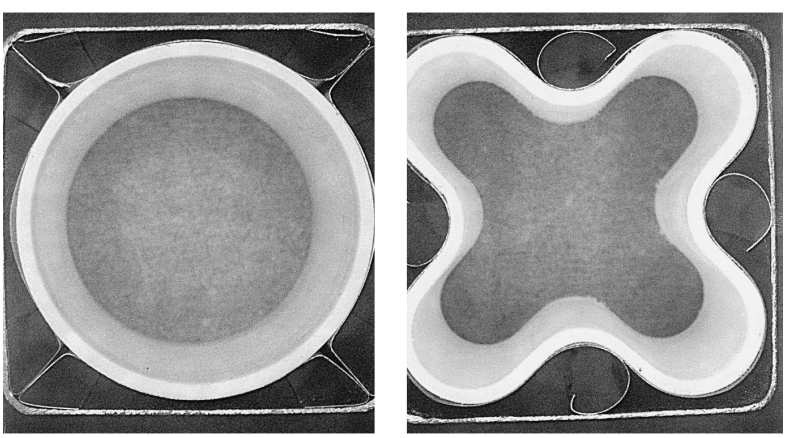

Fig. 2. Comparison of beta alumina tube cross-sections for SL/09 and ML/1G cells.

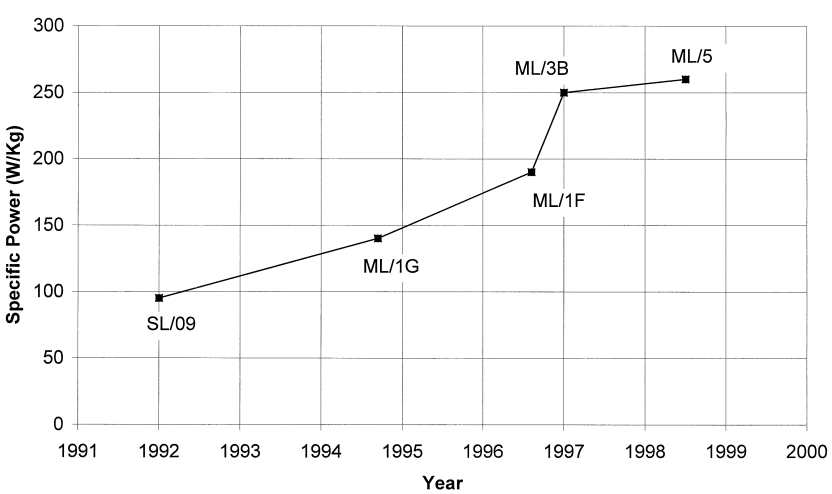

Fig. 3. Comparison of the specific pulse power of ZEBRA cells at 80% DOD.

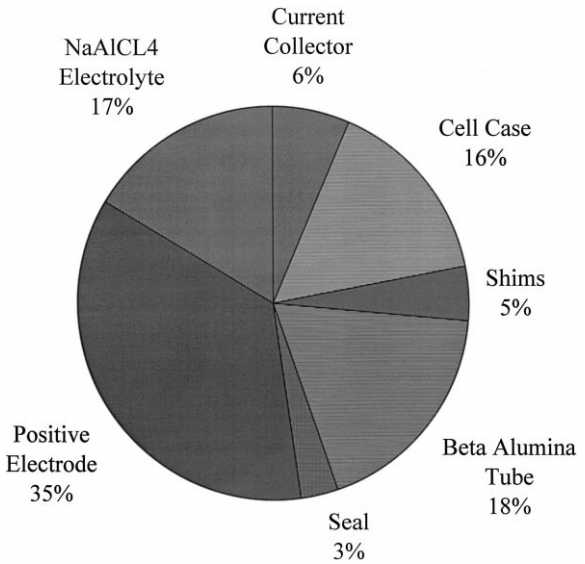

Fig. 4. The weight distribution of the components of the ML/3B Cell.

increasing the available beta alumina surface area by 50% which reduced the resistance contribution of the ceramic proportionately. The resultant ML/1G cells had a pulse power of 180 W per cell at the start of discharge, which reduced to 100 W per cell at 80% DOD.

To reduce the dependence of the pulse power available on the DOD of the cell a second positive electrode reaction was introduced which has a lower potential. Iron was chosen since it had a slightly lower reaction potential and was known to be stable in the ZEBRA system. The cell reactions are:

$$NiCl_2 + Na \rightarrow 2NaCl + Ni \qquad E = 2.58\,V$$

$$FeCl_2 + Na \rightarrow 2NaCl + Fe \qquad E = 2.35\,V$$

For most of the discharge, the system functions as a $Na/NiCl_2$ cell. However, when the working voltage falls below 2.35 V during a high current pulse, the iron reaction augments the main nickel reaction. This occurs at the front of the electrode and the cell therefore has its minimum resistance. When the working voltage recovers above 2.35 V, the iron produced is then reoxidised to iron chloride by the remaining nickel chloride making it available for the next high current discharge. This became the ML/1F cell design which delivered more than 130 W per cell for most of the discharge.

Attention now turned to the current collector which was a twin strip of nickel in the ML/1F cells. By substituting copper cored nickel wire loop for the nickel strip the internal resistance of the cells was reduced by more than 2 mΩ. This ML/3B cell design gave a pulse power of 190 W per cell at 5% DOD and 180 W per cell at 80% DOD.

The current collector in the cell has been developed further by increasing its surface area, reducing its weight, and changing the structure to make cell assembly easier. This has given a further small increase in the pulse power available from these ML/5 cells. Fig. 3 illustrates the improvement in pulse power obtained for the different cell designs.

The next stage of ZEBRA cell development was to increase the energy content of the cells to enable electric vehicles to travel further between recharges.

3. Energy improvement

For the cell reaction:

$$NiCl_2 + 2Na \rightarrow Ni + 2NaCl \qquad E = 2.58\,V$$

the theoretical specific energy is 790 Wh kg^{-1} Fig. 4 indicates the weight distribution of the components that make up the present production cell.

The active materials are contained within the positive electrode which is made up of aluminium, sodium halides, nickel and iron. The role of each is considered in turn.

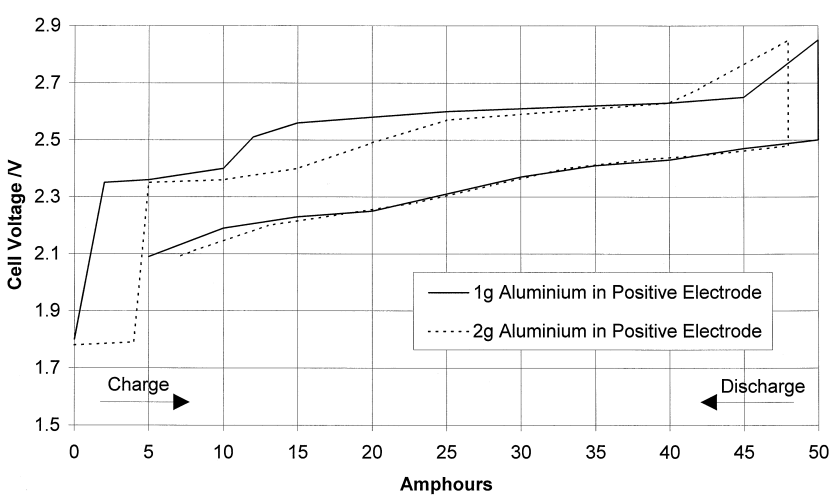

Fig. 5. The effect of different amounts of aluminium in the positive electrode on the charge/discharge profile. Constant current charge of 2.75 to 2.85 A; 12 A constant current discharge.

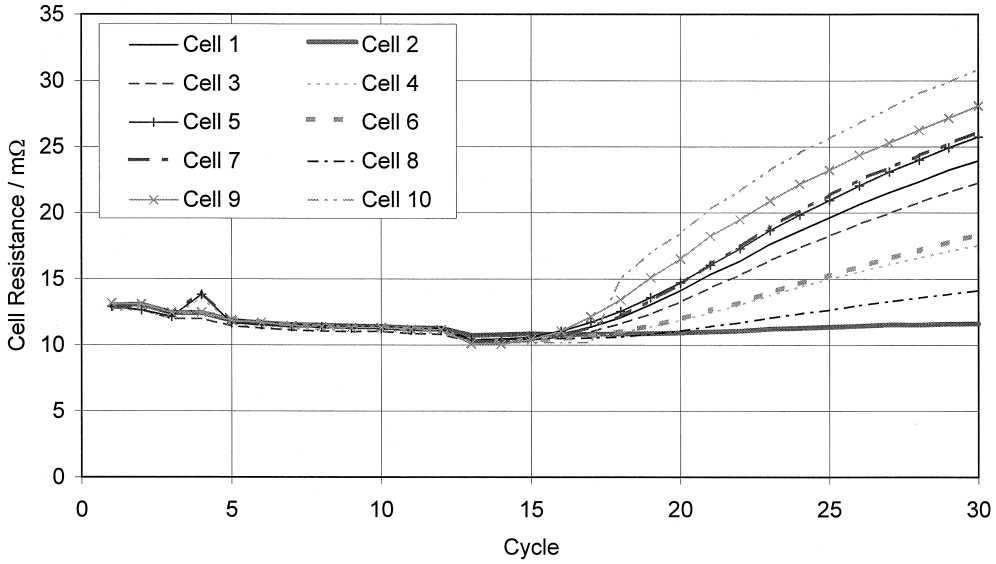

Fig. 6. Graph to show effect of overcharge to 3 V from cycle 12 on BDM 170 cells containing 1 mol% of NaF.

3.1. Aluminium

In practice, it was found convenient to assemble cells in the overdischarged state by including a small amount of aluminium powder with the appropriate amount of sodium chloride in the positive electrode mix. On the first charge the following reaction occurs

$$Al + 4NaCl \rightarrow NaAlCl_4 + 3Na \qquad E = 1.6\,V$$

While this reversible reaction occurs at too low a voltage to be energetically useful, it provides several other useful functions.

(i) Enough pure sodium is generated to prime the sodium electrode shim wick system.

(ii) More sodium tetrachloroaluminate is generated to complement that already added to the positive electrode chamber.

(iii) The porosity generated by the distribution of the aluminium powder in the cathode ensures full charge acceptance on the first charge.

In practice 2 g of aluminium was used which generated 5 g of excess sodium not used during subsequent cell cycling (6 Ah of capacity). Recently, long-term cycling experiments revealed that capacity loss was limited to

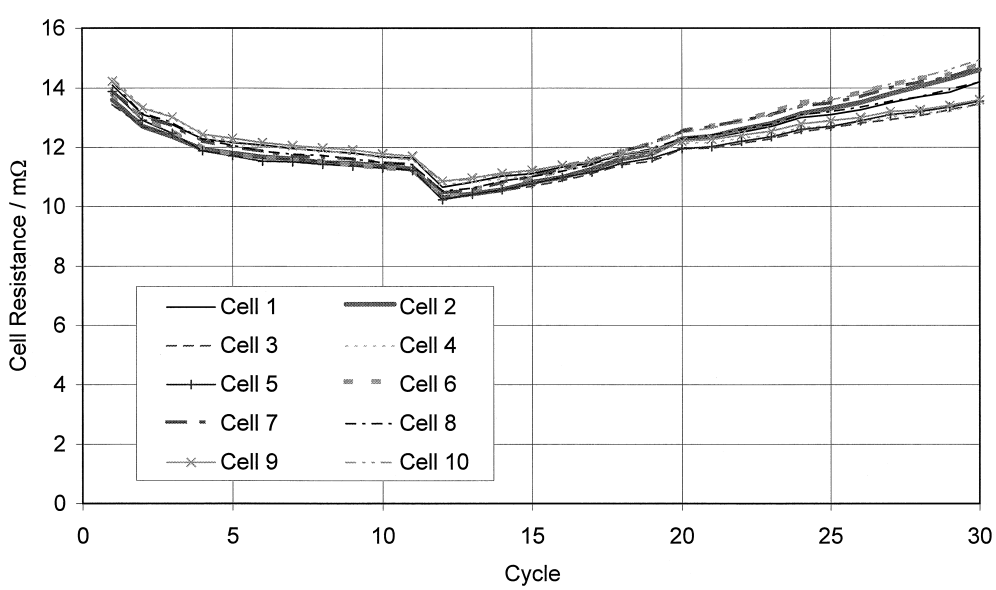

Fig. 7. Graph to show effect of overcharge to 3 V from cycle 12 on BDM 169 cells containing 5 mol% of NaF.

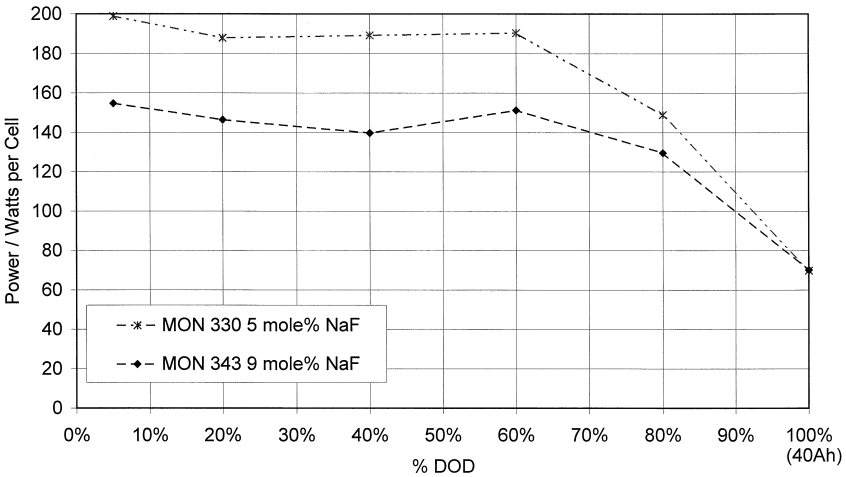

Fig. 8. Graph to show the difference in pulse power between cells with 5 mol% and 9 mol% of NaF.

about 2 Ah [2]. This has allowed the reduction of aluminium and consequently the release of more sodium chloride for the main reaction which improves the cell's useful capacity. This is illustrated in Fig. 5.

3.2. Sodium chloride

This provides the cell's capacity in the reversible cell reaction:

$$M + 2NaCl \rightarrow MCl_2 + 2Na \qquad (M = Ni \text{ or } Fe)$$

All the sodium is generated by electrolysis of the NaCl, which obviates the need to handle sodium metal in the cell assembly stage.

3.3. Sodium fluoride

In ZEBRA cells containing iron, sodium fluoride was an important additive to prevent a rise in internal resistance. $FeCl_2$ is more soluble in the molten salt $NaAlCl_4$ than $NiCl_2$ and under extremes of temperature and voltage it has been shown that iron ions are ion exchanged with beta alumina to cause resistance rise [3]. It is presumed that the solubility of iron in the molten salt is suppressed.

Tolerance to overcharge is also enhanced by NaF doping at low levels. Figs. 6 and 7 show repeated deliberate overcharge to 3 V on modules of 10 cells with two different levels of NaF addition (1 mol% and 5 mol% total halide). At the higher level the cells are clearly more tolerant to overcharge abuse.

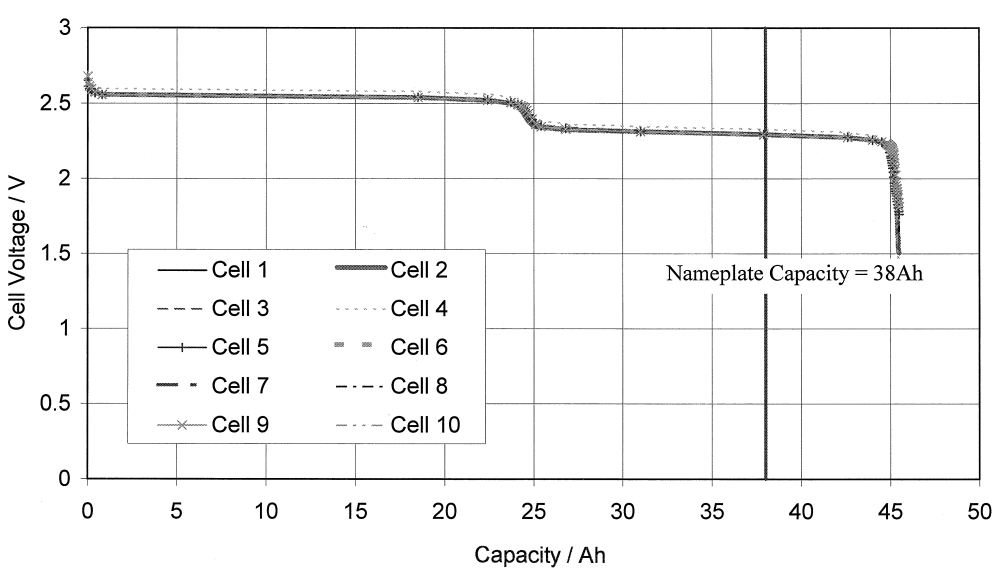

Fig. 9. Graph to show the low rate discharge of Fe-doped cells against Ah discharged.

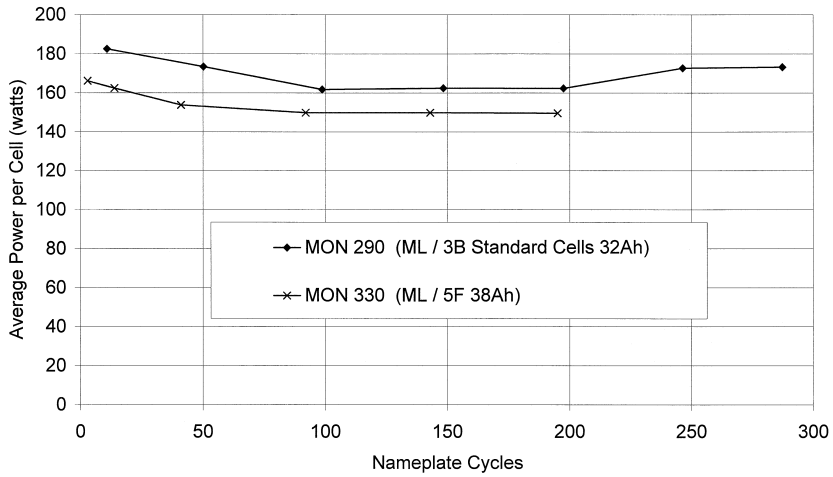

Fig. 10. Comparison of the pulse power at 80% DOD against number of cycles on the DST test regime for ML/3B and ML/5F cells.

Sodium fluoride is a more efficient method of adding capacity to the cell—both gravimetrically and volumetrically:

	NaF	NaCl
Ah from 1 g	0.64	0.46
Ah from 1 cm^3	1.62	0.99

Although on voltage grounds the fluoride reaction is less favourable:

$$NiCl_2 + 2Na \rightarrow 2NaCl + Ni \qquad E = 2.58\,V$$

$$NiF_2 + 2Na \rightarrow 2NaF + Ni \qquad E = 2.39\,V$$

However, work with fluoride-containing chloroaluminate melts [4] indicates mixed ions of the type $AlCl_x\ F_{4-x}^-$ exist and this is likely to be the case in the ZEBRA cell.

Various compositions of positive electrode have been tried where the NaF content has been increased to improve the capacity. Fig. 8 compares the standard pulse power for modules of 10 cells, one with 5 mol% NaF in the cell positive electrode and the other with 9 mol% NaF (of total halide). The higher NaF level gives a higher resistance and hence lower power.

In summary, the addition of sodium fluoride contributes to the useful energy of the cell. Its presence provides a degree of overcharge protection, however at higher levels (9 mol% total halide added) there is evidence that it increases the resistance of the cell.

3.4. Nickel (+iron)

An excess of metal is used, mainly nickel, so that about 30% of the metal is utilised during the charge/discharge reaction. Higher utilisation is possible but this curtails the cycle life [5]. The unused metal maintains electronic con-

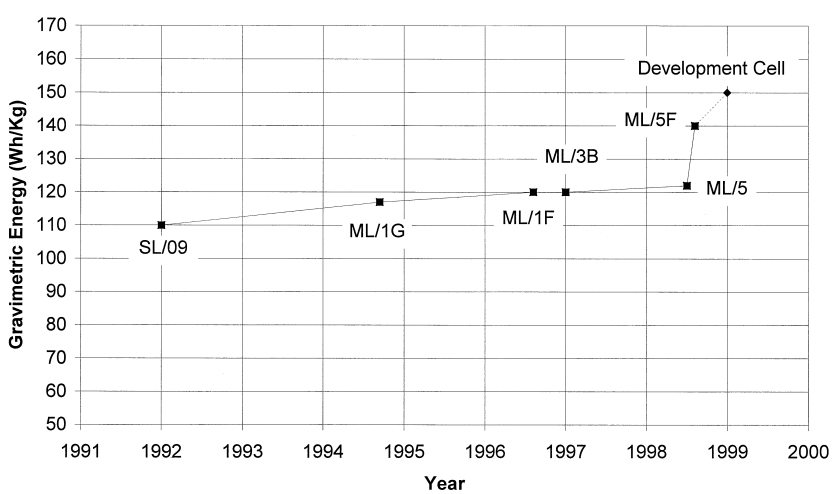

Fig. 11. The improvement in gravimetric energy density of the ZEBRA cell during the current development programme.

ductivity in the electrode. The recent replacement of some of the nickel with iron—to bolster the cell's power—has also lowered the cost of the cell. Fig. 9, showing a low-rate discharge plot for a 10 cell module over the cell's entire capacity, indicates that over the operating range the discharge is mainly due to the reduction of nickel chloride.

By optimising the composition of the positive electrode the nameplate capacity of the cell has been increased from 32 Ah to 38 Ah (the ML/5F cell). Tests are currently ongoing at the battery and module level to establish stability in a dynamic environment that is representative of the discharge duty seen in an electric vehicle. The test involves discharge to 80% DOD using a USABC Dynamic ''Stress test (DST)'', where the battery is regularly pulsed at 80% of its peak specified power value. Every 50 nameplate cycles, the battery is reassessed with a standard pulse power test. Fig. 10 compares the performance of a module of standard ML/3B cells (32 Ah) with a module of ML/5F cells (38 Ah). Power performance at 80% DOD has been stable for more than 200 cycles. Battery results are equally encouraging.

A low-rate discharge on a 10-cell module of the new 38 Ah cells after 387 simulated EV cycles indicates that more than 44 Ah of capacity is still available. Additionally, recent published results [2,6] also show full capacity retention after 1000 cycles, suggesting the unmodified cell is capable of delivering more capacity than that originally specified. Since at 38 Ah the nameplate capacity of the new cell is still only 83% of the theoretical capacity (excluding the aluminium reaction) a further increase to give a 40 Ah cell should be possible.

4. Conclusions

Design changes have produced a new generation of ZEBRA cell with a specific pulse power of 250 W kg^{-1} (capacity 32 Ah, energy 120 Wh kg^{-1}). Further optimisation of the positive electrode has raised the specific energy of the cell to 140 Wh kg^{-1} (38 Ah) but with some sacrifice in power. Fig. 11 shows specific energy improvements over the last 6 years.

It is planned to improve the ohmic resistance of the cell by lowering the resistivity of the beta alumina and this, together with a small increase in the nameplate capacity to 40 Ah, will give a ZEBRA cell with a specific energy of 150 Wh kg^{-1} and a specific power of 250 W kg^{-1} maintained to 80% DOD by the iron booster reaction.

References

[1] J. Coetzer, J.L. Sudworth, EVS-13 Osaka, Japan, 1996.
[2] R.C. Galloway, S. Haslam, 12th IBA Meeting, Annecy-Grenoble, 1998.
[3] P.T. Moseley, R.J. Bones, D.A. Teagle, B.A. Bellamy, R.W.M. Hawes, J. Electrochem. Soc. 136 (5) (1989) 1361–1368.
[4] B. Gilbert, S.D. Williams, G. Mamantov, Inorg. Chem. 27 (13) (1988) 2359–2363.
[5] R.C. Galloway, J. Coetzer, 9th IBA Battery Material Symposium, 1995.
[6] R.N. Bull, W.G. Bugden, S.D. Brooker, R.C. Galloway, W.A. Holmes, EVS-15 Brussels, 1998.